



## Characterization and environmental application of iron-modified zeolite from the Zlatokop deposit

Marin Ugrina<sup>a,\*</sup>, Nediljka Vukojević Medvidović<sup>a</sup>, Aleksandra Daković<sup>b</sup>

<sup>a</sup>Faculty of Chemistry and Technology, Department of Environmental Engineering, University of Split, Teslina 10/V, 21000 Split, Croatia

Tel. +385 21 329454; Fax: +385 21 329461; email: [mugrin@ktf-split.hr](mailto:mugrin@ktf-split.hr)

<sup>b</sup>Institute for Technology of Nuclear and Other Mineral Raw Materials, P.O. Box 390, 11000 Belgrade, Serbia

Received 10 July 2013; Accepted 4 December 2013

---

### ABSTRACT

In this paper, characterization of iron-modified zeolite (IMZ) from the Zlatokop deposit and its potential environmental application has been described. The modification procedure includes treatment of natural zeolite (NZ) with  $\text{Fe}(\text{NO}_3)_3$  in an acetate buffer at  $\text{pH} = 3.6$  followed by treatment with  $\text{NaOH}$  and  $\text{NaNO}_3$ . The properties of NZs and IMZs have been determined by analysis of their chemical composition, specific surface area and by X-ray powder diffraction method (XRPD), scanning electron microscopy-energy dispersive X-ray analysis (SEM-EDS), TG-DTG and FTIR analyses. The chemical behaviour of modified zeolite has been examined in the zeolite-ultrapure water system at adjusted initial  $\text{pH}$  values in the range of 1.71–5.08, and also by determining the zero-point charge. The NZ and IMZ samples have been tested relative to the uptake of zinc ions. The results have shown that the capacity of IMZ samples for zinc ions is three-to-four times higher compared to the NZs. The balance of exchangeable ions before and after zinc uptake confirms an almost complete stoichiometric relation for both zeolite samples indicating ion exchange as the main process. However, in IMZ samples ion exchange takes place inside the zeolite particle and on activated zeolite particle surface.

*Keywords:* Natural zeolite; Iron-modified zeolite; XRPD; SEM-EDS; FTIR; TG-DTG

---

### 1. Introduction

Pollution by hazardous heavy metals presents serious environmental problems throughout the world. Wastewaters from different industries, agriculture, and domestic effluents are sources of their release into the environment [1]. Heavy metals are not biodegradable and tend to accumulate in organisms and soil causing

numerous problems due to their toxicity. Therefore, it is necessary to remove them from water and wastewaters using different methods. The choice of method depends on the type and concentration of heavy metal in water, as well as on the cost of the treatment. Higher heavy metal concentrations are usually removed by precipitation as metal hydroxides. Lower concentrations can be removed by adsorption, ion exchange, ultrafiltration, reverse osmosis, nanofiltration, electrodialysis, etc. [2]. Among these methods, adsorption and ion exchange process are probably the most

---

\*Corresponding author.

attractive due to their high efficiency, and possibility of using low-cost sorbent such as natural zeolite (NZ).

Zeolites are naturally occurring minerals of three-dimensional porous aluminosilicates framework structure with a net negative charge which is neutralized by exchangeable cations ( $\text{Na}^+$ ,  $\text{K}^+$ ,  $\text{Ca}^{2+}$  and  $\text{Mg}^{2+}$ ). Due to the presence of exchangeable cations in the zeolitic structure and the net negative charge of the surface, they have the affinity of ion exchange and adsorption of inorganic cations, but have low or no affinity for anions and organic compounds [3–6]. Therefore, surfactant-modified zeolites have been widely investigated for the uptake of anionic and nonpolar organic compounds [7–9]. Also, many authors have investigated different methods for zeolite surface modification in order to achieve higher sorption properties towards cationic species. Chemical modification with acid, base and salts as well as hydrothermal treatment are the most commonly used treatment methods [5,10]. One of the modifications is conversion into the homoionic form, usually with sodium salts, and it has shown the increase in capacity up to 2.5 times [11,12]. Recently, some authors have modified zeolite with inorganic salts like iron and manganese, and increased its affinity towards metals and other specifically sorbing ions due to larger surface area and increase number of active sites. The increased sorption ability towards anionic and cationic species is common to all methods of zeolite modification [13–26]. Doula and Dimirkou [13–15] have investigated the removal of  $\text{Cu}^{2+}$ ,  $\text{Zn}^{2+}$  and  $\text{Mn}^{2+}$  on a Clin-Fe system prepared according to the method of preparation of pure goethite by treating clinoptilolite with  $\text{Fe}(\text{NO}_3)_3$  in the presence of  $\text{KOH}$  at  $70^\circ\text{C}$  during 60 h. They have reported that this treatment method led to an increase in the number of active sites on its external and internal surface. The sorption capacity of Clin was  $7.69\text{ mg g}^{-1}$  for  $\text{Mn}^{2+}$ ,  $71.3\text{ mg g}^{-1}$  for  $\text{Zn}^{2+}$  and  $13.6\text{ mg g}^{-1}$  for  $\text{Cu}^{2+}$ , whereas in the Clin-Fe system it was 27.12, 94.8 and  $37.5\text{ mg g}^{-1}$ , respectively.

Han et al. [16] have investigated  $\text{Cu}^{2+}$  removal on iron oxide-coated zeolite prepared by treating zeolite with  $\text{FeCl}_3$  by addition of  $\text{NaOH}$  at  $80^\circ\text{C}$ , followed by heating of the obtained sample at  $500^\circ\text{C}$  during 4 h. They have reported that coated zeolite surfaces were occupied by newborn iron oxides, so that the equilibrium sorption capacity for  $\text{Cu}^{2+}$  increases from  $3.88\text{ mg g}^{-1}$  for NZ to  $5.14\text{ mg g}^{-1}$  for iron oxide-coated zeolite. Kragović et al. [17] have investigated the removal of lead onto Fe(III)-modified zeolite prepared by treating NZ with  $\text{FeCl}_3$  and  $\text{KOH}$  at  $25^\circ\text{C}$ , followed by the aging of the suspension for 20 days according to the combined methods for preparation of pure

goethite. They have found two times higher capacity of Fe(III)-modified zeolite compared to the starting material, equalling  $133\text{ mg g}^{-1}$  for the Fe(III)-modified zeolite and  $66\text{ mg g}^{-1}$  for the NZ. Zeolite modified with iron salts has shown the ability to bind anionic species [20–25]. Jeon et al. [18], Habuda-Stanić et al. [19] and Li et al. [20] have investigated the removal of arsenic anionic species on iron-modified zeolite (IMZ) prepared by a similar procedure which includes treatment with Fe(III) salts followed by the treatment with  $\text{NaOH}$ . They have reported that the adsorption of arsenic species occurs on ferrihydrite hydroxide groups, but the obtained capacity for removal of arsenic species was not significant  $\approx 0.1\text{ mg g}^{-1}$ . Šiljeg et al. [21] have also investigated the removal of arsenic species on Fe-modified zeolite prepared by treatment with  $\text{NaCl}$  for 24 h at  $70^\circ\text{C}$  followed by treatment with  $\text{FeCl}_3$  at pH 3.6 for 24 h at  $70^\circ\text{C}$ . They have obtained a significant removal capacity for As(III) and As(V) species on Fe-modified clinoptilolite, which was equal to  $20.2\text{ mg g}^{-1}$  for Fe-modified zeolite originating from the Donje Jesenje deposit, Croatia and  $27.1\text{ mg g}^{-1}$  for Fe-modified zeolite originating from the Vranjska Banja deposit, Serbia.

The aim of this study is to prepare a new IMZ with improved sorption capacity towards heavy metal ions. The characterization and chemical behaviour of NZ and IMZ have been determined and IMZ has been tested in respect to the uptake of zinc ions.

## 2. Materials and methods

### 2.1. Preparation and physico-chemical characterization of zeolite samples

The NZ originated from the Zlatokop deposit, Vranjska Banja, Serbia. The sample was milled and sieved to two particle size fractions of  $<0.043\text{ mm}$  and  $0.6\text{--}0.8\text{ mm}$ , rinsed with ultrapure water, dried at  $60^\circ\text{C}$  and stored in the desiccator.

The IMZ was prepared from NZ of both particle sizes.  $20.0\text{ g}$  of each NZ was shaken with  $100\text{ ml}$  of freshly prepared  $0.1\text{ mol l}^{-1}\text{ Fe}(\text{NO}_3)_3\cdot 9\text{H}_2\text{O}$  in an acetate buffer at  $\text{pH}=3.6$ , for 2 h in the incubator shaker at the room temperature. After filtration, the sample was shaken with  $90\text{ ml}$  of  $1\text{ mol l}^{-1}\text{ NaOH}$  for an hour. Thereafter, the zeolites were treated for an hour at  $50^\circ\text{C}$  with  $50\text{ ml}$  of 4%  $\text{NaNO}_3$  and than with 50% of ethanol. The prepared IMZs were dried for 24 h at  $40^\circ\text{C}$ , kept in the desiccator [19,26].

The chemical composition of NZs and IMZs was determined by the classical chemical analysis of aluminosilicates and Table 1 shows the results.

The specific surface area (SSA) and the pore volume properties for the solid materials (NZs and

IMZs) were measured by a Micromeritics Gemini 2360 Surface Area Analyser, with the degassing of samples during 12 h, at 20°C. The results are presented in Table 2.

The qualitative X-ray powder diffraction method (XRPD) of all samples was performed on a Phillips PW-1710 diffractometer with monochromatic Cu-K $\alpha$  radiation, in the range of  $2\theta=4-60^\circ$ , with a step scan of  $0.02^\circ$ .

Scanning electron microscopy (SEM) analysis and energy dispersive X-ray analysis (EDS) of NZ and IMZ have been performed on a JEOL JSM-6610 microscope. Electron microscopy was performed at magnifications of 500 and 50,000. The analysis of SEM images was combined with electron diffraction analysis in the way that semi-quantitative EDS elemental analysis is performed on a marked surface or point on the SEM image.

Infrared spectra of NZs and IMZs were measured on a Thermo Nicolet FTIR 6500 spectrometer. The samples were prepared by the standard KBr pellets method.

Thermal analysis of NZs and IMZs was performed using a Perkin Elmer STA 6000. Samples were heated (20–1,000°C) in an air atmosphere, at a heating rate of  $10^\circ\text{C min}^{-1}$ .

## 2.2. Chemical behaviour of IMZ sample

The chemical behaviour of IMZ in ultrapure water at different pH values has been examined by mixing 5 g of IMZ (0.6–0.8 mm) with 500 ml of ultrapure water in a

700-ml closed glass vessel with a double wall, at 200 rpm and at  $20 \pm 1^\circ\text{C}$ . The initial pH values of the ultrapure water (pH = 5.08, 3.80, 2.85 and 1.71) were adjusted by addition of  $0.1 \text{ mol l}^{-1}$  HCl. The pH values of suspensions were measured continuously during 24 h. At defined time intervals, portions of 10 ml of the suspension were taken (the total amount of the suspension taken did not exceed 5% of the entire suspension volume) and centrifuged, and the liquid phase was analysed. The concentrations of released exchangeable cations  $\text{Na}^+$ ,  $\text{K}^+$ ,  $\text{Ca}^{2+}$  and  $\text{Mg}^{2+}$  from IMZ were determined by ion chromatography and Si and Al were determined by UV–vis spectrophotometry.

The point of zero charge ( $\text{pH}_{\text{pzc}}$ ) of natural and IMZ was determined using the aqueous solution of  $\text{KNO}_3$  ( $0.001-0.1 \text{ mol l}^{-1}$ ) as a background electrolyte by the batch technique [9]. The initial pH value ( $\text{pH}_i$ ) of each solution was adjusted by addition of  $0.1 \text{ mol l}^{-1}$  KOH or  $0.1 \text{ mol l}^{-1}$   $\text{HNO}_3$ . The 50 ml of each solution with different initial pH values (pH range 2–12) was shaken with 0.1 g of each sample for 24 h at room temperature. After equilibration, suspension was filtered and pH was measured in the filtrate.

## 2.3. Zinc uptake test

The examinations of zinc uptake were carried out by shaking 1 g of NZ or IMZ with 100 ml of aqueous solutions containing initial zinc concentrations ( $c_0 = 1.98-13.29 \text{ mmol l}^{-1}$ ). Experiments were performed at the room temperature, using the batch technique for 24 h. After equilibration, the suspensions

Table 1  
Chemical composition of zeolite samples

Sample, mm	Content, wt. %								
	SiO <sub>2</sub>	Al <sub>2</sub> O <sub>3</sub>	Fe <sub>2</sub> O <sub>3</sub>	CaO	MgO	K <sub>2</sub> O	Na <sub>2</sub> O	TiO <sub>2</sub>	Loss of ignition
NZ <0.043	66.57	13.13	2.30	3.85	0.56	1.17	1.27	–	11.05
NZ 0.6–0.8	65.40	14.00	2.16	3.56	0.85	1.10	1.50	0.32	11.09
IMZ <0.043	60.10	14.84	3.36	4.00	0.85	1.04	3.73	0.34	11.81
IMZ 0.6–0.8	62.80	13.90	2.22	3.85	0.80	0.94	3.68	0.17	11.56

Table 2  
SSA and pore properties for zeolite samples

Sample, mm	Specific surface area, $\text{m}^2 \text{ g}^{-1}$	Pore volume, $\text{cm}^3 \text{ g}^{-1}$	Pore diameter, nm
NZ 0.6–0.8	20.171	0.065	4.171
NZ <0.043	22.561	0.047	4.141
IMZ 0.6–0.8	19.903	0.083	3.943
IMZ <0.043	25.705	0.114	4.144

were filtered and concentrations of removed zinc ions as well as concentrations of released exchangeable cations and iron ions were determined by ion chromatography.

### 3. Results and discussion

#### 3.1. Physico-chemical characterization of zeolite samples

Based on the results of chemical analysis presented in Table 1, the element composition of NZ and IMZ has been calculated [21,27,28] and shown in Table 3.

The results have shown that the preparation of IMZ caused a slight decrease of the Si/Al ratio and a slight increase of iron content, which was more evident with the lower particle size. Among exchangeable cations, calcium dominates in the NZ sample. In the IMZ sample, the amount of sodium increased significantly, while the amount of other exchangeable cations remained almost unchanged. This means that the total amount of exchangeable cations in the IMZ sample has increased.

The SSAs of NZ and IMZ of the particle size of 0.6–0.8 mm have remained almost unchanged, but the pore volume has increased. At the particle size of < 0.043 mm, IMZ has a slightly higher surface area, but a significantly higher pore volume. The increase in pore volume can be attributed to some impurities dissolving in a slightly acid medium. At pH = 3.6, the iron exists in cationic species ( $\text{Fe}(\text{H}_2\text{O})_6^{3+}$ ,  $[\text{Fe}(\text{H}_2\text{O})_5\text{OH}]^{2+}$ ,  $[\text{Fe}(\text{H}_2\text{O})_4(\text{OH})_2]^+$ ,  $\text{Fe}_2(\text{OH})_2^{4+}$ ) with dominating  $[\text{Fe}(\text{H}_2\text{O})_5\text{OH}]^{2+}$ , and they can be sorbed on the negative zeolite surface [29,30]. The addition of NaOH enables hydrolysis of iron species previously sorbed on the particle surface and leads to formation of various Fe hydroxocomplexes species [26,29]. These species are probably carriers of negative charge to which sodium ions bind in higher amounts. Also, at the basic condition  $\equiv\text{Si}-\text{OH}-\text{Al}\equiv$  zeolite surface groups lose their hydrogen ions and become negatively charged, which also contributes to the increase of the negative surface charge of zeolite [15]. The higher

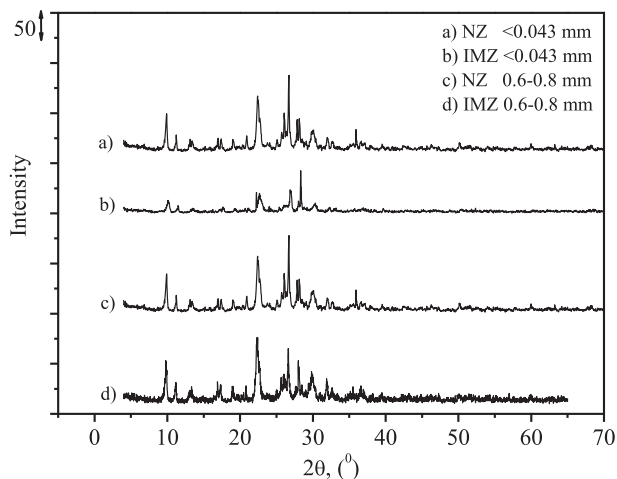


Fig. 1. XRPD spectra for NZ and IMZ.

amount of sodium had been previously confirmed by chemical analysis.

From the XRPD analysis of the NZ and IMZ samples presented in Fig. 1, the characteristic peaks of clinoptilolite were recognized for both samples, but a slight decrease of the peak intensity is observed for IMZ. Lower peak intensity is more pronounced for particle sizes of <0.043 mm and can be attributed to the slight decrease in the crystallinity of NZ after modification process.

Scanning electron microscopy-energy dispersive X-ray analysis (SEM-EDS) analyses of NZ and IMZ zeolite have been performed by analysing the marked surfaces on the images (Fig. 2). Mass percentage values of the detected element on the marked zeolite surface are shown for three spectrums for NZ and five spectrums for IMZ in Tables 4 and 5. Only one spectrum for each SEM image is presented in Fig. 2.

The results show uniform element composition between three spectrums for NZ and five spectrums for IMZ. The comparison of mean mass percentage values of detected element on marked zeolite surfaces obtained for NZ and IMZ indicates that the percentage

Table 3  
Element quantity of zeolite samples

Sample, mm	Element quantity, $\text{mmol g}^{-1}$							
	Na	K	Ca	Mg	Fe	Al	Si	Si/Al
NZ <0.043	0.356	0.216	0.597	0.121	0.250	2.239	9.631	4.301
NZ 0.6–0.8	0.421	0.203	0.552	0.184	0.235	2.390	9.472	3.963
IMZ <0.043	1.181	0.197	0.641	0.190	0.378	2.614	8.983	3.436
IMZ 0.6–0.8	1.054	0.177	0.610	0.177	0.247	2.421	9.280	3.833

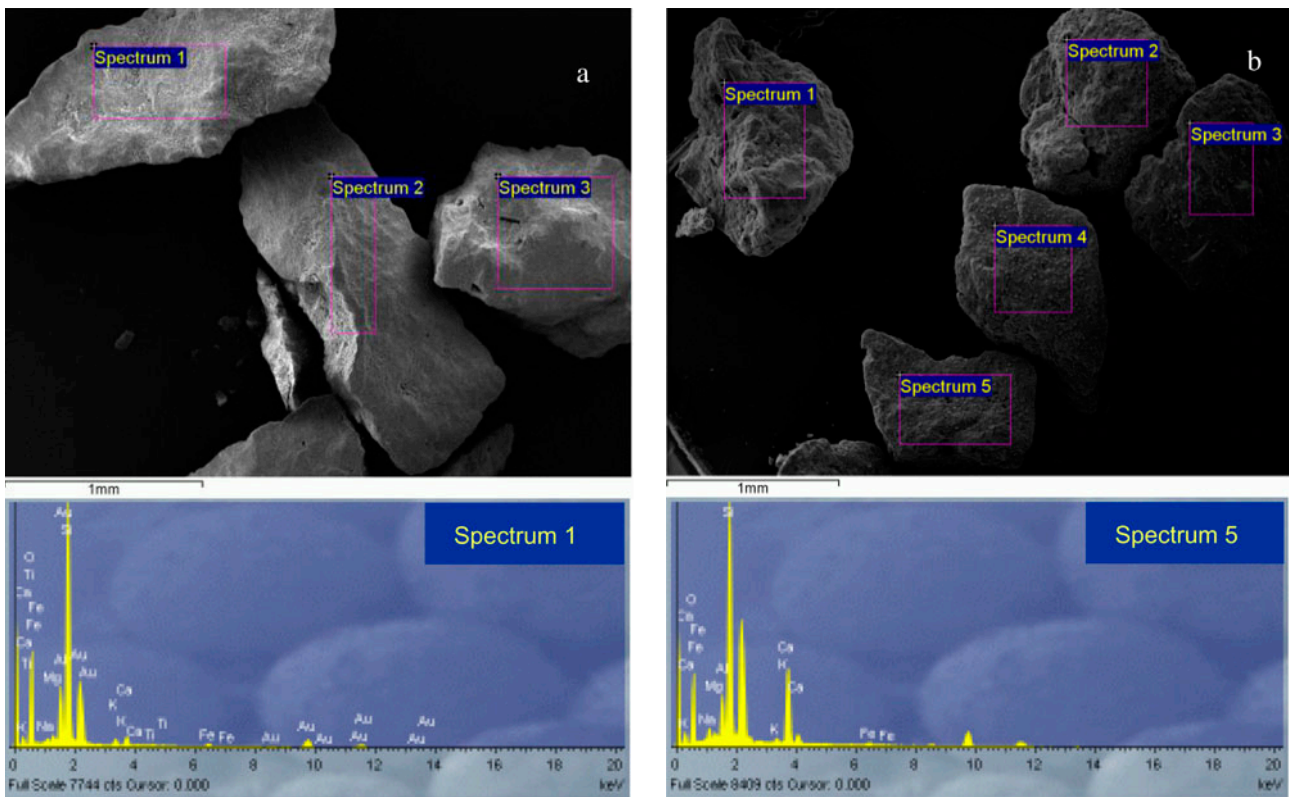


Fig. 2. SEM image and EDS analysis of: (a) NZ and (b) IMZ of particle size 0.6–0.8 mm.

Table 4

Mass percentage values of the detected element on the marked zeolite surface for three spectrums for NZ

Element	Spectrum 1 mass%	Spectrum 2 mass%	Spectrum 3 mass%	Mean mass%
Na	0.95	0.80	0.82	0.86
K	1.44	1.38	0.99	1.27
Ca	2.31	2.82	3.04	2.72
Mg	0.89	0.73	0.65	0.76
Fe	2.07	1.63	1.64	1.78
Si	35.02	36.00	36.59	35.87
Al	7.15	6.29	6.23	6.56
O	49.63	49.83	50.05	49.84

of iron slightly increases for IMZ. Among exchangeable cations on the IMZ surface, the percentage of sodium and calcium increases three and six times, respectively. In order to expand the analysis of the surface on IMZ zeolites, SEM image was done at magnification of 50,000  $\times$  (Fig. 3).

The SEM images of NZ show typical plates for clinoptilolite, while the surface covering is evident from its modified form. Additional SEM and EDS analyses of the IMZ sample have been performed at magnification

of 500  $\times$  (Fig. 4). Mass percentage values of detected element on marked point at the zeolite surface have been presented for three spectrums in Table 6.

The result shows that formed particles on the IMZ surface mainly consisted of calcium. Moreover, the amount of calcium is extremely higher compared to its amount shown in Table 5. The higher content of calcium could be attributed to the basic conditions during the modification procedure, in which calcium exchanged with sodium precipitates on the zeolite surface.

The TG thermograms of the IMZ and NZ sample (Fig. 5) show similar total weight loss.

The first weight loss (60–150°C) is due to weakly bound water. The second weight loss (150–250°C) is due to water bound to exchangeable cations [28]. This peak was less evident for the IMZ samples, indicating a lower interaction energy between water molecules and exchangeable cations (mostly Na<sup>+</sup>), and thus their lower thermal stability. The third weight loss (450–500°C) is also more evident in the IMZ samples and corresponds to the structural water. The IMZ samples show the fourth weight loss (670–720°C) which can be attributed to the decomposition of trace amounts of calcium carbonate formed during the

Table 5

Mass percentage values of the detected element on the marked zeolite surface for five spectrums for IMZ (Fig. 2b)

Element	Spectrum 1 mass%	Spectrum 2 mass%	Spectrum 3 mass%	Spectrum 4 mass%	Spectrum 5 mass%	Mean mass%
Na	2.62	2.90	1.58	2.25	2.04	2.28
K	0.71	0.59	0.76	0.75	0.83	0.73
Ca	13.28	18.40	13.58	18.47	16.59	16.05
Mg	0.69	0.42	0.46	0.60	0.75	0.58
Fe	2.76	1.83	2.56	1.67	1.60	2.08
Si	28.72	26.53	30.05	26.98	28.29	28.11
Al	5.27	5.06	4.89	4.83	4.77	4.96
O	45.63	44.27	46.12	44.46	45.14	45.12

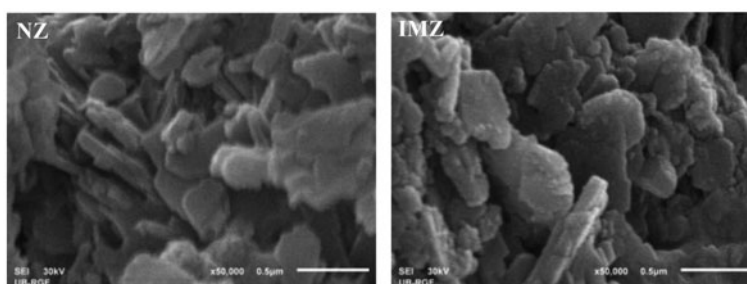


Fig. 3. SEM of NZ and IMZ of particle size 0.6–0.8.

modification process [31]. Specifically, the SEM-EDS analysis of the IMZ samples has shown increased amounts of calcium on the surface, probably existing as calcium carbonate. During the modification procedure,  $\text{Na}^+$  ions replace  $\text{Ca}^{2+}$  ions from the zeolite structure and, in alkaline conditions, form calcium hydroxide on the zeolite edges and broken bonds which, in the presence of carbon dioxide, convert into calcium carbonate. The formation of calcium carbonate corresponds to the mechanism of heterogeneous nucleation, so that the growth of a new solid phase takes place in the presence of foreign particles in a supersaturated solution.

Fig. 6 shows the FTIR spectrums of NZ and IMZ samples. FTIR spectrums for all the samples are very similar. Hydroxyl bands, O–H stretching, ( $3,621\text{--}3,625\text{ cm}^{-1}$ ), slightly increases for the IMZ samples of both particle sizes and corresponds to the increase in the zeolite water. The strong band is due to the water-bending mode appearing at  $1,640\text{--}1,646\text{ cm}^{-1}$ , and becoming more intensive for the IMZ sample. The weakening and noticeable absences of the structure sensitive band at  $1,140\text{ cm}^{-1}$  (asymmetric T–O stretching) in the IMZ sample of lower particle size indicate a decrease in crystallinity, which can be due to decrease in silicon content during the modification procedure [16,32,33].

Additionally, the FTIR spectrum of lower particle sizes shows a band at  $1,384\text{ cm}^{-1}$ , indicating that the product contains traces of nitrate adsorbed on the zeolite surface during the modification procedure [26].

### 3.2. Chemical behaviour of IMZ

The investigation of the chemical behaviour of IMZ in the IMZ-ultrapure water system at different initial pH values is useful for understanding the sorption mechanism of metal cations on zeolite. The chemical behaviour of IMZ was estimated in the IMZ-ultrapure water system at different initial pH values by continuous measuring of pH and the concentrations of released cations Na, K, Ca, Mg, Si and Al in the solution after the contact of IMZ with ultrapure water. The experimental results are shown in Figs. 7–9.

As can be seen from Fig. 7, at the initial pH = 2.85–5.08, a rapid increase of the final pH values is observed, while at the initial pH = 1.71, the final pH remains unchanged. This increase of pH values is probably due to the ion exchange between  $\text{H}^+$  ions from the solution and exchangeable cations from IMZ according to the following reaction [34]:

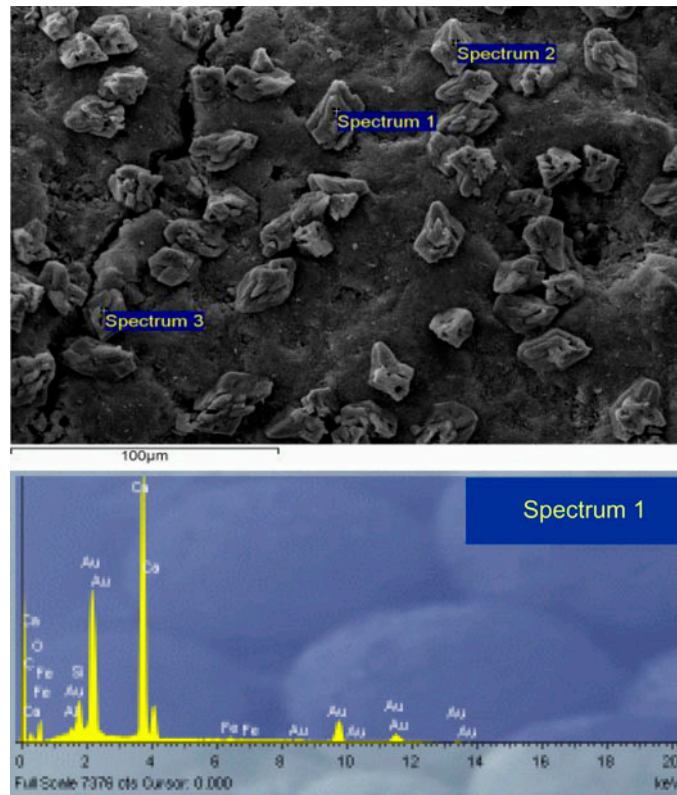
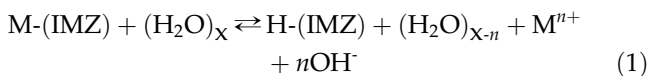


Fig. 4. SEM image and EDS analysis of the particles formed on IMZ surface.

Table 6  
Mass percentage values of the detected element on three marked points on IMZ zeolite surface

Element	Spectrum 1 mass%	Spectrum 2 mass%	Spectrum 3 mass%	Mean mass%
Na	0.00	0.00	0.00	0.00
K	0.00	0.00	0.00	0.00
Ca	62.32	68.96	70.45	67.25
Mg	0.32	0.00	0.00	0.11
Fe	1.13	0.00	0.00	0.38
Si	4.27	1.27	0.67	2.07
Al	0.80	0.42	0.00	0.41
O	31.15	29.35	28.88	29.79



where  $M^{n+}$  –  $Na^+$ ,  $K^+$ ,  $Ca^{2+}$ ,  $Mg^{2+}$  and IMZ – iron-modified zeolite.

This effect is less evident at the initial pH value of 2.85, as released  $OH^-$  ions are only partially neutralized and the equilibrium  $pH=8$  is reached in 300 min (Fig. 7).

At  $pH=1.71$ , the suspension pH remained unchanged during 24 h. This is due to the high initial  $H^+$  concentration at which, beside ion exchange with  $H^+$  ions, partial degradation and dissolution of zeolite particles occurs. Specifically, in a strong acid medium, elimination of exchangeable cations takes place, as well as dealumination accompanied by the degradation of the zeolitic structure [35,36] (Figs. 8 and 9).

The surface of zeolitic particles in electrolyte solutions is electrically charged and, depending on pH, the zeolite surface can be positive, neutral and negative. The pH value at which the charge of zeolite surface is equal to zero is defined as the point of zero charge ( $pH_{pzc}$ ) [9]. The  $pH_{pzc}$  can play a significant role in understanding the sorption mechanism of inorganic and organic species at the solid/solution interface. Thus, the  $pH_{pzc}$  of NZ and IMZ was determined by measuring the  $pH_f$  as a function of  $pH_i$  at different ionic strengths of electrolytes (Fig. 10).

The final pH values of suspensions for both samples increase until reaching the plateau. The plateaus of the curves corresponds to  $pH_{pzc}$ , and is equal  $6.8 \pm 0.1$  for NZ and  $9.8 \pm 0.1$  for IMZ. The length of the plateau is from 5 to 9 for NZ, while extended from 4 to 10 for IMZ. The  $pH_{pzc}$  of both samples is

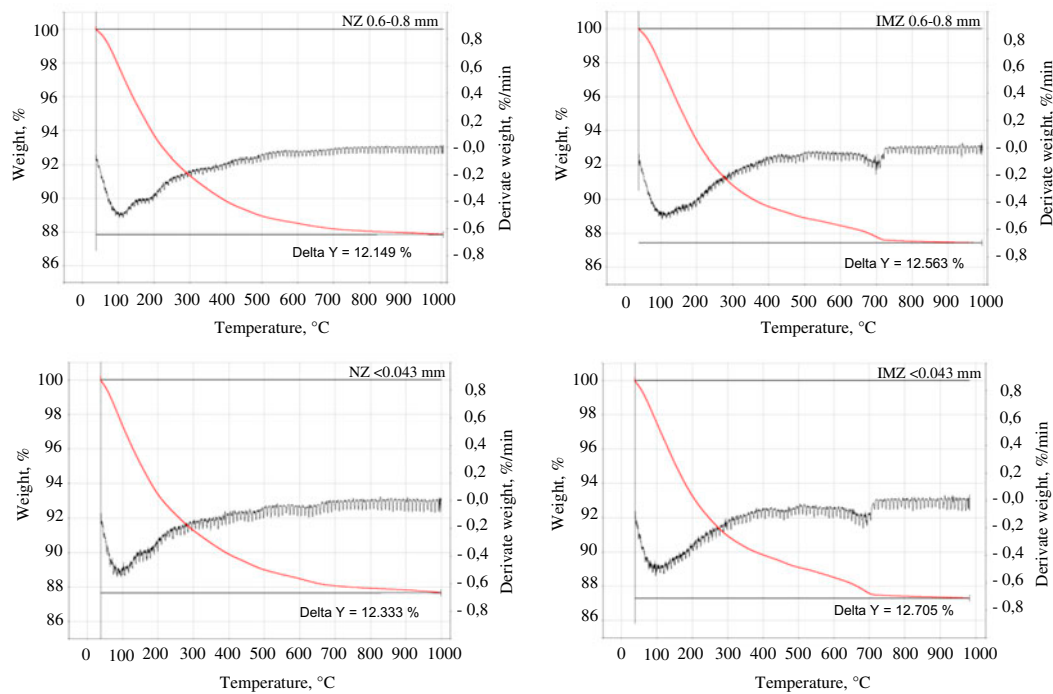


Fig. 5. TG-DTG analysis of NZ and IMZ.

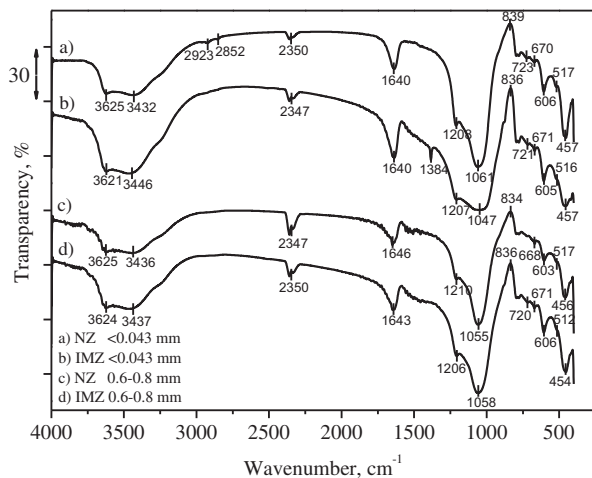


Fig. 6. FTIR spectra of NZ and IMZ.

the same for all three electrolyte concentrations, which indicates that the  $pH_{pzc}$  for this material is independent of the ionic strength [9]. The most important is that  $pH_{pzc}$  of IMZ is approximately three pH units higher compared to the NZ. The increase of  $pH_{pzc}$  for IMZ, most probably, results in an increase in the number of negative charge.

### 3.3. Zinc uptake on NZ and IMZ

These experiments were continued with preliminary examinations of zinc removal from aqueous solutions on NZ and IMZ and Fig. 11 shows the obtained results. For both zeolite samples, zinc uptake increases with the increase of the initial zinc concentration and with the decrease of the particle size.

The results for zinc removal by NZ and IMZ of both particle sizes have been fitted to linearized Langmuir adsorption isotherms. The calculated parameters are shown in Table 7.

The value of the calculated correlation coefficient indicates the applicability of the Langmuir isotherm. This allows for calculating the capacity of a zeolite sample for zinc ions from the Langmuir parameter  $q_0$ . The results show that the capacity of IMZ for both particle sizes is 3–4 times higher than the capacity of NZ for zinc ions ( $0.418 \text{ mmol g}^{-1}$  vs.  $0.127 \text{ mmol g}^{-1}$  for higher particle size, respectively, and  $0.438 \text{ mmol g}^{-1}$  vs.  $0.142 \text{ mmol g}^{-1}$  for lower particle size, respectively). After saturation with zinc ions, the final pH shows a tendency of neutralization, even the final pH value in suspensions of IMZ-ultrapure water reached pH of around 10. This indicates the buffering ability of the IMZ sample and it is being accepted for use in *in situ* remediation of wastewater.

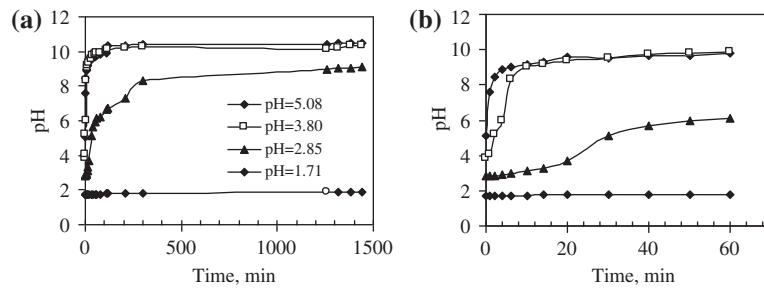


Fig. 7. Continuous measurement of pH in the IMZ-ultrapure water system at different initial pH values: (a) in the abscissa range of 1,440 min and (b) in the abscissa range of 60 min.

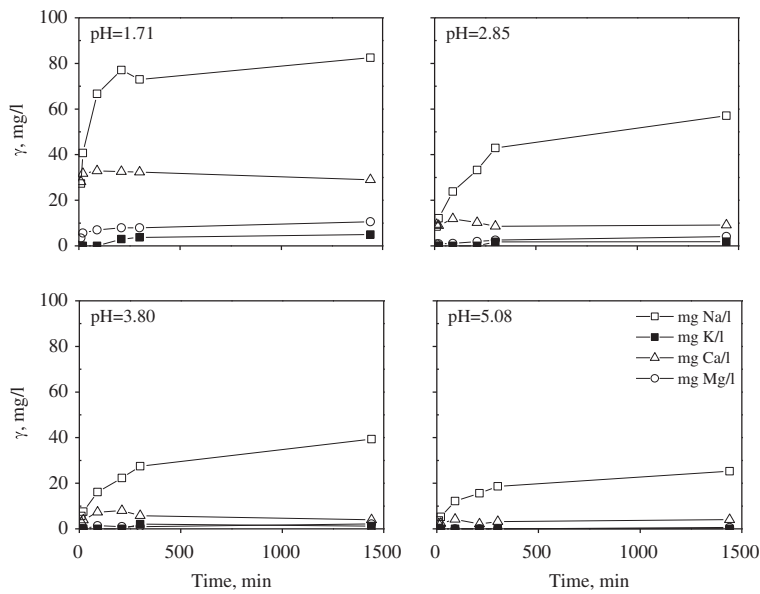


Fig. 8. Concentrations of  $\text{Na}^+$ ,  $\text{K}^+$ ,  $\text{Ca}^{2+}$  and  $\text{Mg}^{2+}$  in the IMZ-ultrapure water system during 24 h at different initial pH values.

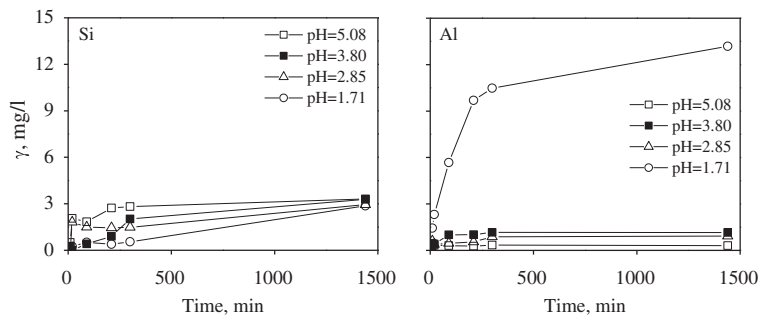


Fig. 9. Concentrations of  $\text{Si}^{4+}$  and  $\text{Al}^{3+}$  in the IMZ-ultrapure water system during 24 h at different initial pH values.

The chemical composition of NZ and IMZ of particle size of 0.6–0.8 mm after saturation with zinc ions has been analysed and Table 8 shows the amounts of elements.

The total amount of  $\text{Na}^+$ ,  $\text{K}^+$ ,  $\text{Ca}^{2+}$  and  $\text{Mg}^{2+}$  in the IMZ sample compared to NZ has increased from 1.360 to 2.018  $\text{mmol g}^{-1}$  (2.096 vs. 2.805 meq), indicating higher metal uptake in the IMZ sample. After saturation

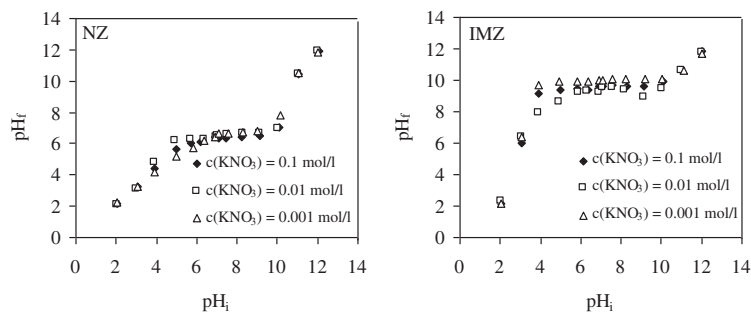


Fig. 10.  $pH_f$  vs.  $pH_i$  of NZ and IMZ at different concentrations of background electrolyte.

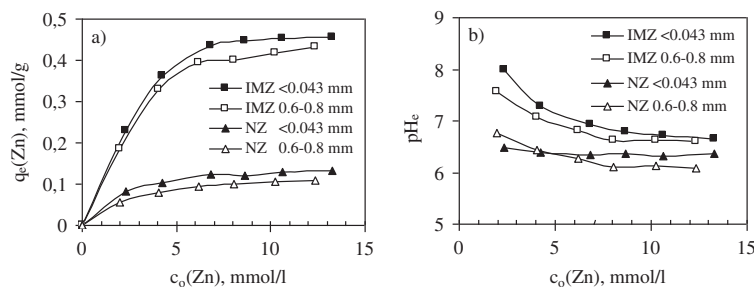


Fig. 11. Quantity of zinc uptake on NZ and IMZ for both particle sizes (a) and equilibrium pH values vs. initial zinc concentration for both particle sizes (b).

Table 7  
Calculated parameters of Langmuir isotherms

Sample	Particle size, mm	Langmuir isotherm parameters		
		$K_L$ , $l\text{ mmol}^{-1}$	$q_0$ , $\text{mmol g}^{-1}$	$R^2$
NZ	0.6–0.8	0.070	0.127	0.999
	<0.043	0.132	0.142	0.981
IMZ	0.6–0.8	2.902	0.418	0.993
	<0.043	17.301	0.438	0.950

of the IMZ sample with zinc ions, the amount of sodium decreases from  $1.054$  to  $0.586\text{ meq g}^{-1}$ , while the amount of zinc removed on IMZ equals  $0.500\text{ meq g}^{-1}$ . It indicates that zinc has been replaced with an almost stoichiometric amount of sodium ( $0.468$  vs.  $0.500\text{ meq g}^{-1}$ ). The amount of zinc removed by IMZ compared to NZ is three-to-four times higher ( $0.081$  vs.  $0.250\text{ mmol g}^{-1}$ ), which agrees with the results obtained by Langmuir isotherm (Table 7).

The SEM-EDS analysis of the sample after zinc uptake, NZZn and IMZZn zeolite for particle size of  $0.6\text{--}0.8\text{ mm}$ , has been performed by analysing three marked surfaces on the image for NZZn and five for IMZZn. Mean mass percentage values of the detected element on the marked zeolite surface for NZZn and

IMZZn have been calculated and presented in Fig. 12, with two spectra for each sample.

The SEM-EDS analysis has indicated that the amount of zinc on the IMZZn surface is  $\approx 13$  times more compared to the NZZn sample and is homogeneously distributed over the five analysed surfaces of different particles. This has confirmed that the modification changes the zeolite surface probably by increasing the negatively charged active sorption places due to the treatment of NZ in a Fe(III) solution in the acidic medium, followed by the treatment with NaOH and  $\text{NaNO}_3$ . These negatively charged sorption active places are occupied by bound Na ions from the solution where a part of sodium ions is exchanged with calcium ions, and they are dominant exchangeable cations. Both of these effects are responsible for a 3–4 times higher amount of exchanged zinc ions on IMZ compared to NZ.

The relations between the concentrations of  $\text{Na}^+$ ,  $\text{K}^+$ ,  $\text{Ca}^{2+}$  and  $\text{Mg}^{2+}$  ions leaving the zeolite structure and concentrations of Zn ions entering the zeolite structure have been calculated for different initial zinc concentrations and are presented in Fig. 13.

Among all exchangeable cations, for the IMZ samples, concentrations of released Na ions are 2–8 times higher compared to the sum of other exchangeable cations and are dependent on the initial

Table 8

Comparison of element quantity of zeolite samples before and after saturation with zinc

Sample, mm	Element quantity, mmol g <sup>-1</sup>								
	Na	K	Ca	Mg	Fe	Al	Si	Zn	Si/Al
NZ 0.6–0.8	0.421	0.203	0.552	0.184	0.235	2.390	9.472	0.003	3.963
IMZ 0.6–0.8	1.054	0.177	0.610	0.177	0.247	2.421	9.280	0.002	3.833
NZZn 0.6–0.8	0.346	0.203	0.576	0.173	0.230	2.573	9.368	0.081	3.641
IMZZn 0.6–0.8	0.586	0.177	0.565	0.159	0.268	2.498	9.339	0.252	3.739

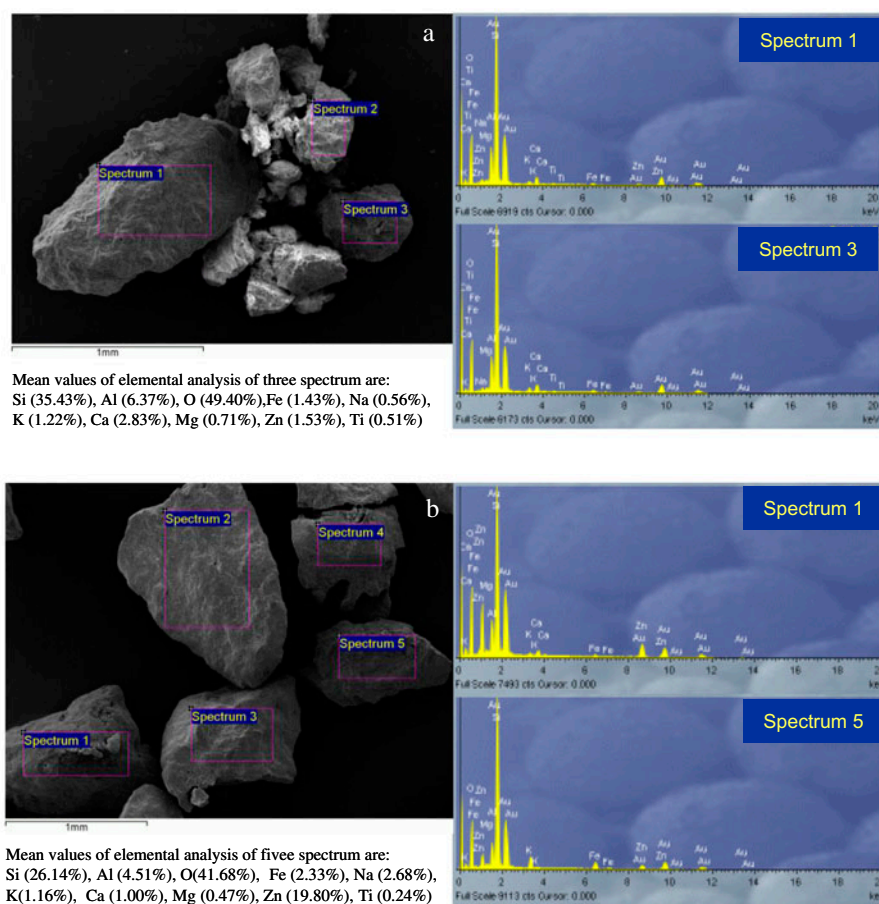


Fig. 12. SEM image and EDS analysis of NZ and IMZ after saturation with zinc ions: (a) NZZn and (b) IMZZn, particle size 0.6–0.8 mm.

zinc concentrations. The balance of ions confirms an almost complete stoichiometric relation for NZ and IMZ of both particle sizes. This indicates that ion exchange is the main mechanism of binding of zinc ions, while for IMZ ion exchange takes place inside the zeolite particle and on activated-zeolite particle surface.

#### 4. Conclusion

The modification procedure of the NZ to IMZ changes the composition of exchangeable cations and physical properties particularly on the particle surface. The modification of NZ in a Fe(III) solution at pH = 3.6 enables the sorption of Fe(III) cation species on the

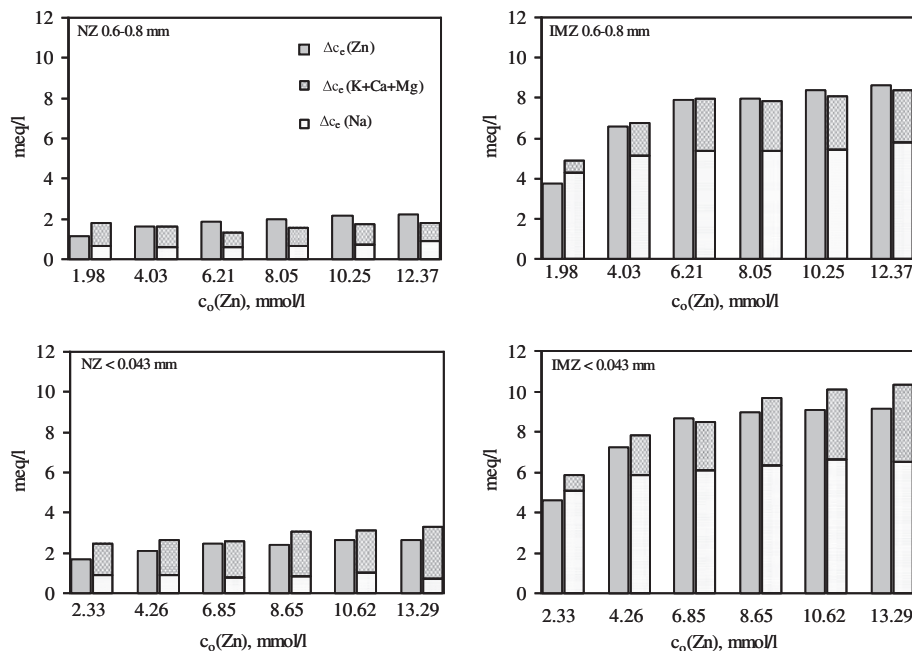


Fig. 13. Relationship between the concentration of Zn bound and released exchangeable cations in the solution as a function of initial zinc concentration. Note:  $\Delta c_e = c_{\text{initial}} - c_{\text{final}}$ .

negative zeolite surface. The treatment in NaOH enables the hydrolysis of bound iron species, resulting in the formation of various Fe hydroxocomplex species which are carriers of negative charge that are neutralized by sodium ions. The basic condition leads to deprotonation of the  $\equiv\text{Si}-\text{OH}-\text{Al}\equiv$  zeolite surface groups, which also contributes to the increase of the negative zeolite surface charge. The increased amount of sodium ions was confirmed by chemical analysis, while the increase in the negative surface charge was confirmed by determination of the point of zero charge which is three pH units higher for IMZ compared to NZ.

The SEM-EDS analysis of the zeolite particle surface shows a significant difference in elemental composition compared to the chemical analysis of whole grains for the NZ and IMZ samples. This difference is particularly evident in increased calcium and sodium content on the IMZ particle surface.

The removal of zinc ions on IMZ is about 3–4 times higher compared to that on NZ, the particle size does not effect the removal capacity, and sodium ions mostly dominate among other ions leaving the IMZ structure. The elemental analysis of SEM images of IMZ after metal ions uptake has shown a higher content of Zn and its homogeneous distribution over the five analysed surfaces of different particles. This confirms that the modification causes changes on the surface of zeolite particles and contributes to higher removal capacity of IMZ.

These results indicate IMZ as a promising material with increased abilities for heavy metals removal. However, further experiments should be performed to investigate the equilibrium and kinetics in binary and multicomponent solutions as well as regeneration of saturated IMZ and possible multiple reuse of the same modified zeolite.

#### Acknowledgements

We are thankful to the Ministry of Science, Education and Sports of the Republic of Croatia, which has been financing the project 011-0000000-2239 a part of which is presented in this paper. These investigations are also conducted as a part of the bilateral project between the Republic of Serbia and the Republic of Croatia.

#### References

- [1] P.C. Nagajyoti, K.D. Lee, T.V.M. Sreekanth, Heavy metals, occurrence and toxicity for plants: A review, *Environ. Chem. Lett.* 8 (2010) 199–216.
- [2] F. Fu, Q. Wang, Removal of heavy metal ions from wastewaters: A review, *J. Environ. Manage.* 92 (2011) 407–418.
- [3] W. Shi, H. Shao, H. Li, M. Shao, S. Du, Progress in the remediation of hazardous heavy metal-polluted soils by natural zeolite, *J. Hazard. Mater.* 170 (2009) 1–6.
- [4] M. Minceva, R. Fajgar, L. Markovska, V. Meshko, Comparative study of  $\text{Zn}^{2+}$ ,  $\text{Cd}^{2+}$ , and  $\text{Pb}^{2+}$  removal from water solution using natural clinoptilolitic zeolite

- and commercial granulated activated carbon. Equilibrium of adsorption, *Sep. Sci. Technol.* 43 (2008) 2117–2143.
- [5] S. Wang, Y. Peng, Natural zeolites as effective adsorbents in water and wastewater treatment, *Chem. Eng. J.* 156 (2010) 11–24.
- [6] N. Widiastuti, H. Wu, M. Ang, D. Zhang, The potential application of natural zeolite for greywater treatment, *Desalination* 218 (2008) 271–280.
- [7] G.M. Haggerty, R.S. Bowman, Sorption of chromate and other inorganic anions by organo-zeolite, *Environ. Sci. Technol.* 28 (1994) 452–458.
- [8] Z. Li, R.S. Bowman, Regeneration of surfactant-modified zeolite after saturation with chromate and perchloroethylene, *Water Res.* 35 (2001) 322–326.
- [9] A. Daković, M. Kragović, G.E. Rottinghaus, Ž. Sekulić, S. Milićević, S.K. Milonjić, S. Zarić, Influence of natural zeolitic tuff and organozeolites surface charge on sorption of ionizable fumonisin B<sub>1</sub>, *Colloids Surf., B* 76 (2010) 272–278.
- [10] K. Elaiopoulos, Th Perraki, E. Grigoropoulou, Monitoring the effect of hydrothermal treatments on the structure of a natural zeolite through a combined XRD, FTIR, XRF, SEM and N<sub>2</sub>-porosimetry analysis, *Micropor. Mesopor. Mater.* 134 (2010) 29–43.
- [11] L. Lin, Z. Lei, L. Wang, X. Liu, Y. Zhang, C. Wan, D.-J. Lee, J.H. Tay, Adsorption mechanisms of high-levels of ammonium onto natural and NaCl-modified zeolites, *Sep. Sci. Technol.* 103 (2013) 15–20.
- [12] S.R. Taffarel, J. Rubio, On the removal of Mn<sup>2+</sup> ions by adsorption onto natural and activated Chilean zeolites, *Miner. Eng.* 22 (2009) 336–343.
- [13] M.K. Doula, Removal of Mn<sup>2+</sup> ions from drinking water by using clinoptilolite and a clinoptilolite-Fe oxide system, *Water Res.* 40 (2006) 3167–3176.
- [14] A. Dimirkou, Uptake of Zn<sup>2+</sup> ions by a fully iron-exchanged clinoptilolite. Case study of heavily drinking water samples, *Water Res.* 41 (2007) 2763–2773.
- [15] M.K. Doula, Synthesis of a clinoptilolite-Fe system with high Cu sorption capacity, *Chemosphere* 67 (2007) 731–740.
- [16] R. Han, L. Zou, X. Zhao, Y. Xu, F. Xu, Y. Li, Y. Wang, Characterization and properties of iron oxide-coated zeolite as adsorbent for removal of copper(II) from solution in fixed bed column, *Chem. Eng. J.* 149 (2009) 123–131.
- [17] M. Kragović, A. Daković, Ž. Sekulić, M. Trgo, M. Ugrina, J. Perić, G.D. Gatta, Removal of lead from aqueous solutions by using the natural and Fe(III)-modified zeolite, *Appl. Surf. Sci.* 258 (2012) 3667–3673.
- [18] C. Jeon, K. Baek, J. Park, Y. Oh, S. Lee, Adsorption characteristics of As(V) on iron-coated zeolite, *J. Hazard. Mater.* 163 (2009) 804–808.
- [19] M. Habuda-Stanić, B. Kalajdžić, M. Kuleš, N. Velić, Arsenite and arsenate sorption by hydrous ferric oxide/polymeric material, *Desalination* 229 (2008) 1–9.
- [20] Z. Li, J. Jean, W. Jiang, P. Chang, C. Chen, L. Liao, Removal of arsenic from water using Fe-exchanged natural zeolite, *J. Hazard. Mater.* 187 (2011) 318–323.
- [21] M. Šiljeg, Š. Stefanović, M. Mazaj, N. Tušar, I. Arčon, J. Kovač, K. Margeta, V. Kaučić, N. Logar, Structure investigation of As(III)- and As(V)-species bound to Fe-modified clinoptilolite tuffs, *Micropor. Mesopor. Mater.* 118 (2009) 408–415.
- [22] M.J. Jiménez-Cedillo, M.T. Olguín, Ch. Fall, Adsorption kinetic of arsenates as water pollutant on iron, manganese and iron-manganese-modified clinoptilolite-rich tuffs, *J. Hazard. Mater.* 163 (2009) 939–945.
- [23] M. Noroozifar, M. Khorasani-Motlagh, P. Ahmadzadeh Fard, Cyanide uptake from wastewater by modified natrolite zeolite-iron oxyhydroxide system: Application of isotherm and kinetic models, *J. Hazard. Mater.* 166 (2009) 1060–1066.
- [24] G. Du, Z. Li, L. Liao, R. Hanson, S. Leick, N. Hoepfner, W.-T. Jiang, Cr(VI) retention and transport through Fe(III)-coated natural zeolite, *J. Hazard. Mater.* 221–222 (2012) 118–123.
- [25] Y. Sun, Q. Fang, J. Dong, X. Cheng, J. Xu, Removal of fluoride from drinking water by natural stilbite zeolite modified with Fe(III), *Desalination* 277 (2011) 121–127.
- [26] U. Schwertmann, R.M. Cornell, *Iron Oxides in the Laboratory*, Wiley-VCH, Weinheim, 2000.
- [27] R.T. Pabalan, Thermodynamics of ion exchange between clinoptilolite and aqueous solution of Na<sup>+</sup>/K<sup>+</sup> and Na<sup>+</sup>/Ca<sup>2+</sup>, *Geochim. Cosmochim. Acta* 58 (1994) 4573–4590.
- [28] P. Castaldi, L. Santona, C. Cozza, V. Giuliano, C. Abbruzzese, V. Nastro, P. Melis, Thermal and spectroscopic studies of zeolites exchanged with metal cations, *J. Mol. Struct.* 734 (2005) 99–105.
- [29] L.D. Benefield, J.F. Judkins, B.L. Weand, *Process Chemistry for water and wastewater treatment*, Prentice-Hall, Englewood Cliffs, NJ, 1982.
- [30] L. Borgnino, M.J. Avena, C.P. De Pauli, Synthesis and characterization of Fe(III) montmorillonites for phosphate adsorption, *Colloids Surf., A* 341 (2009) 46–52.
- [31] I. Halikia, L. Zoumpoulakis, E. Christodoulou, D. Prattis, Kinetic study of the thermal decomposition of calcium carbonate by isothermal methods of analysis, *Eur. J. Miner. Process. Environ. Prot.* 1 (2001) 89–102.
- [32] M.S. Joshi, V.V. Joshi, A.L. Choudhari, M.W. Kasture, Structural studies of natural heulandite using infrared spectroscopy, *Mater. Chem. Phys.* 48 (1997) 160–163.
- [33] W. Mozgawa, M. Sitarz, M. Rokita, Spectroscopic studies of different aluminosilicate structures, *J. Mol. Struct.* 511–512 (1999) 251–257.
- [34] M. Wark, W. Lutz, G. Schulz-Ekloff, A. Dyer, Quantitative monitoring of side products during high loading of zeolites by heavy metals via pH measurements, *Zeolites* 13 (1993) 658–662.
- [35] A. Filippidis, A. Godelitsas, D. Charistos, P. Misaelides, A. Kassoli-Fournaraki, The chemical behavior of natural zeolites in aqueous environments: Interactions between low-silica zeolites and 1M NaCl solutions of different initial pH-values, *Appl. Clay Sci.* 11 (1996) 199–209.
- [36] E. Dumitriu, C. Cobzaru, V. Huela, A. Rotariu, S. Oprea, Dealuminated natural zeolites for application in catalytic processes with formation of C–C bonds. 1. Modification of the natural clinoptilolite by dealumination, *Rev. Chim. (Bucuresti)*, 60 (2009) 297–300.